Publisher version : 10.1021/acsenergylett.0c00156

Influence of the subcell properties on the fill-factor of two-terminal perovskite-silicon tandem solar cells

Mathieu Boccard and Christophe Ballif.*

Photovoltaics and Thin-Film Electronics Laboratory (PV-lab), Institute of Microengineering (IMT), École Polytechnique Fédérale de Lausanne (EPFL), Rue de la Maladière 71b, CH-2002 Neuchâtel, Switzerland.

AUTHOR INFORMATION

Corresponding Author

*Mathieu.boccard@epfl.ch.

ABSTRACT. The performance of a tandem solar cell depends on the performance of its constituting subcells. Although this dependency is theoretically straightforward for open-circuit voltage (Voc) and short-circuit current, it is indirect for fill-factor (FF) and thus for efficiency. We study here with simple simulations the effect on the tandem performance of each-subcell FF by varying systematically their series resistance, parallel resistance, and local defect. We demonstrate

that series resistance impacts strongly FF for single-junction devices but marginally for tandem devices, the opposite holding for parallel resistances (shunting). We show that localized defects will be most stringent to the tandem device when they occur in the current-limiting subcell. There is thus no obvious correlation between FFs of a tandem device and of its subcells. Finally, we compare two bottom-cell designs and highlight the importance of using high-Voc bottom cell to reach high tandem efficiencies.

TOC GRAPHICS

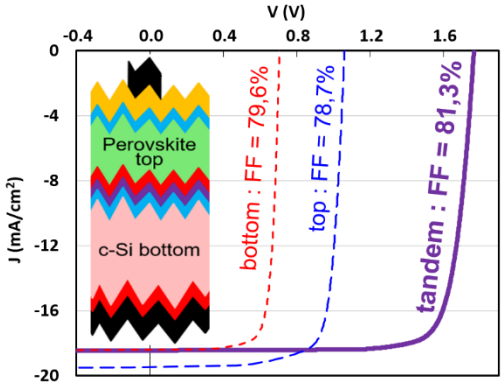

MAIN TEXT

The serial connection in two-terminal tandem solar cells prevents the detailed independent analysis of each single-junction sub-cell. This renders difficult the identification of the causes limiting performance of the full device, which is necessary to guide development. Several strategies were however shown to enable indirect assessment of sub-cell properties.[1–5] Globally, short-circuit current density (Jsc) of the tandem correspond to the limiting one of the two subcells (each sub-cell Jsc can be measured with spectral response using bias light in a satisfactory manner), and open-circuit voltage (Voc) of good devices equals the sum of each sub-

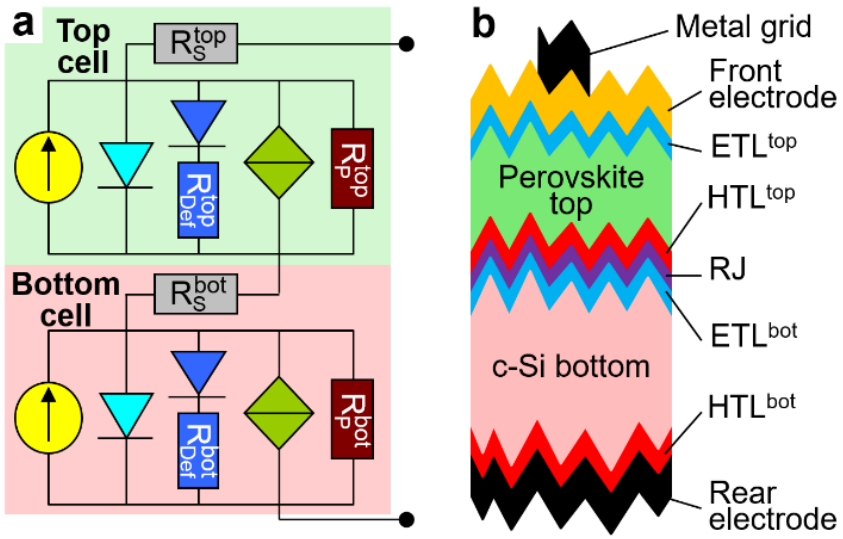

FIG. 1 a) Equivalent circuit of the simulated devices, highlighting the three resistance varied in each subcell. The darker blue diode represents locally defective areas and the green diamonds additional recombination elements. b) Sketch of the considered device. HTL and ETL stand for hole- and electron-transport layer, respectively, and the superscript relates to the sub-cell it applies to (top or bottom)

cells Voc at the corresponding illumination. However, for fill factor (FF), there is no straightforward correspondence between the one of each sub-cells and the one of the tandem device. Furthermore, current matching was shown to also play a role in determining the FF of a tandem device.[6–11]

With the raise of perovskite-silicon tandem devices with impressive efficiency values (>25%),[12–15] the impact of performance loss in individual subcells on the tandem performance is an important point to target most efficient device integration in this specific system. In particular, although the importance of using a high-efficiency bottom-cell to reach high performance has been clearly demonstrated,[16] the best silicon-cell architecture is still not clearly identified with high tandem-cell efficiencies demonstrated with multiple strategies.[12,17,18] This contribution aims at discussing the FF of tandem devices in relation to the FF of each constituent. Using for each sub-cell a very simple two-diode model with similar elements,[19] and a serial connection of the

two in the tandem (Fig. 1), we discuss the effect of changing in each subcell the series resistance, the parallel resistance, and the influence of local-defects, on the FF of the single-junction and tandem device. We notably show that a few percent change of FF in a given subcell can have either a negligible effect or a huge impact on the FF of the tandem device depending on the origin of this FF change.

In our modelling we use typical values reflecting the properties of perovskite/Silicon tandem devices. The values used for each parameter are listed in tuning *the* parameters of this defect diode and the value of R_{defect}, one can modify the FF without affecting the Voc or Jsc, and reproduce the oftentimes experimentally observed performance drop originating solely from poor FF and non-attributable to series or parallel resistance (R_S or R_P). Examples of fits of the current-voltage characteristic (reverse-scan) of the recent high-efficiency fully textured perovskite/silicon tandem device from Sahli et al.[12] are given in supporting information, together with a discussion on the uniqueness of such fit.

Table 1 and discussed further below, and Table 2 shows the resulting solar-cell metric extracted from the simulated current-voltage (IV) characteristics. To make this model more general, a recombination element (green diamond in Figure 1a) is introduced in addition to the usual diodes and resistances as suggested for thin-film silicon devices, and also proven useful for crystalline-silicon devices.[19,20] However, this parameter is not limiting in high-efficiency devices since good-enough values for built-in voltage and mobility-lifetime product are usually achieved. Such conditions were chosen here, and not varied throughout the study, so that this element is actually not affecting the device performance in any condition.

The detrimental impact of local areas of high recombination is simulated using a very bad diode quenched by a resistance directly in series (R_{defect}). This model was shown accurate for modeling multiple defects in solar cells, from grain-boundaries in polycrystalline absorbers,[21] to edge effects,[22] to texture-induced imperfections.[23] Physically, this additional resistance accounts for the fact that the defective areas cover a small fraction of the overall device area, connected to the good areas through a non-zero lateral resistance and with a non-zero contact resistance.[22–24] A high value for this resistance could also mimic efficient lateral separation between the good areas and bad areas, as obtained with a non-conductive recombination junction.[25,26] Mathematically, by tuning the parameters of this defect diode and the value of R_{defect}, one can modify the FF without affecting the Voc or Jsc, and reproduce the oftentimes experimentally observed performance drop originating solely from poor FF and non-attributable to series or parallel resistance (R_S or R_P). Examples of fits of the current-voltage characteristic (reverse-scan) of the recent high-efficiency fully textured perovskite/silicon tandem device from Sahli et al.[12] are given in supporting information, together with a discussion on the uniqueness of such fit.

Table 1 Default parameters used in the simulations

	top cell	bottom cell	unit
temperature (T)	298	298	K
built-in voltage (Vbi)	1.5	1	V
cell thickness (L)	0.25	150	µm
Mobility.lifetime (µ.τ)	0.000008	0.1	cm^2/V
diode saturation current (J0)	1.0E-17	1.5E-13	A/cm^2
diode ideality factor (n)	1.2	1.1	-
defects diode saturation current (J02)	0.1	0.1	$\mu A/cm^2$
defects diode ideality factor	3	2	-
Rdefects	0.2	0.3	$k\Omega.cm^2$
parallel resistance (Rp)	20	100.6	$k\Omega.cm^2$
series resistance (Rs)	2	0.6	$\Omega.cm^2$

photogenerated current (Jph)	25	40	mA/cm^2

In our simple exemplary simulations, poor properties were chosen for the "defects diode," and only the value of the defects resistance was changed to tune the influence of areas of high recombination on the overall device performance. A low resistance leads to a strong effect of these defects and thus a low FF, whereas increasing this resistance mitigates the influence and leads to improved FF. A higher defect-diode ideality factor was used for the perovskites to accommodate for the larger variability observed in the FF values of these devices. Fig. 2 shows the IV characteristic of the nominal perovskite device, and the influence of degrading each one of the resistance on the shape of the IV curve for this single-junction device. Using the model of Fig. 1, we reproduced the reverse-scan IV curve of the recent high-efficiency perovskite/silicon tandem device from Sahli et al., as shown in supplementary information.

In the following, the value of the series resistance, parallel resistance and defect resistance is varied in both the perovskite and the c-Si device. We then report the effect of varying these resistances on the FF of each single-junction device alone, on the FF of the single-junction operating in a tandem configuration (i.e. with a photocurrent of 20 mA/cm^2 in lieu of 25 mA/cm^2 or 40 mA/cm^2), and on the FF of the perovskite/silicon tandem device. For the latter, since matching plays a significant role as will be discussed later, three values for the mismatch between the top and bottom cell are compared: -1 mA/cm^2, 0 mA/cm^2 and 1 mA/cm^2. The effect of mismatch on the Jsc, FF and efficiency of the tandem device with default parameters (listed in Table 1) is shown in Figure 3 and matches experimental data.[11] An efficiency > 27% can be reached across a range of mismatch values. Note that the best efficiency is not reached for perfectly matched conditions, but for a slight bottom-limitation. Although less marked than for the thin-film silicon case, for which even the minimal FF was shifted away from matched conditions,[10] this stems from the higher voltage and lower parallel resistance for the top cell.[27]

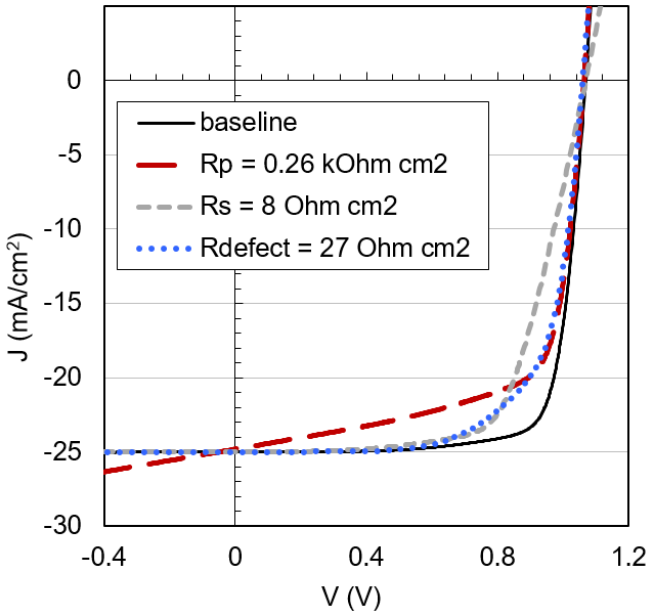

Figure 2 Simulated IV curves of a single-junction perovskite device using the baseline parameters, and of a perovskite device having either the series, parallel or defect resistance worsened (increased for Rs and decreased of the other two).

Table 2 IV parameters simulated using the device parameters from Table 1. Tandem is matched in this case.

	Perovskite single	c-Si single	Top cell	Bottom cell	Matched tandem
Voc (mV)	1069	728	1061	708	1769
Jsc (mA/cm^2)	25.0	39.9	20.0	20.0	19.9
FF (%)	78.9	79.6	78.7	79.6	79.2
Efficiency (%)	**21.1**	**23.1**	**16.7**	**11.2**	**27.9**
Roc (Ω.cm^2)	3.3	1.3	3.6	2.1	5.7
Rsc (kΩ.cm^2)	18.0	9.3	18.3	17.1	25.1

Fig. 4 shows the FF for the single-junction device alone, the single-junction operating in the tandem device (with lower photogenerated current), and the tandem device itself (for three matching conditions) when varying the value of the series resistance parallel resistance and defect resistance in the perovskite solar cell (a-c) or crystalline silicon bottom cell (d-e).

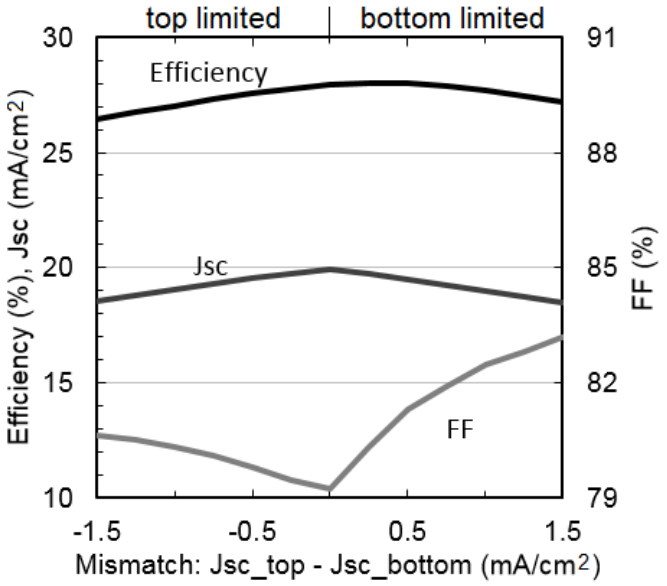

FIG. 3 Simulated efficiency, Jsc and FF of a tandem device as a function of the matching condition.

A first observation from FIG. 4 is that all curves are distinct, confirming the intuition that the FF of each device is influenced differently by a given modification in simulation input. Another striking information is that FF is best for most conditions in the bottom-limited case. This is also observed in Fig. 3 with a steeper FF increase when mismatching towards bottom limitation than top limitation. This stems from the default model assumptions, with better properties for the c-Si solar cell, as is experimentally observed. The top-limited case outperforms other matching conditions only for unrealistically low parallel resistance for the bottom cell (Fig. 4e) or very low-defect top cells (high values for the defect resistance in Fig. 4c). The matched case leads to the worst FF in all conditions (except for strongly shunted bottom cell with Rp < 2kOhm cm^2, or top cell with Rp < 3 kOhm cm^2).

Concerning series resistance (Fig. 4a and d), the impact scales with the impedance of the device: Due to the low impedance at maximum power point of 15 Ohm cm^2, series resistance affects the FF of the c-Si more strongly than the one of the perovskite cell (impedance of 40 Ohm cm^2). When considering each individual cell in a tandem configuration (i.e. with 20 mA/cm^2 of photocurrent instead of 40 mA/cm^2 for the c-Si cell and 25 mA/cm^2 for the perovskite cell), the influence of the series resistance on FF decreases. In the tandem device, the influence of series resistance is identical for all three matching conditions, and is independent from the cell to which it is attributed in the model. This last observation is trivial since we consider a series-connected tandem device. Also, in actual tandem devices, the electrode design is usually different from the single-junction cases, making additional series resistance happening only in the tandem structure likely to occur. This is one of the limitations of FF of actual tandem devices such as the one from Sahli et al.

Conversely, the impact of varying the value of the parallel or defect resistances is strongly dependent on the matching condition, and on the subcell to which this resistance applies. Generally, the tandem device will be most influenced by modifications applied to its limiting subcell. As shown by the yellow curve in Fig. 4b, a bottom-limited tandem will be insensitive to

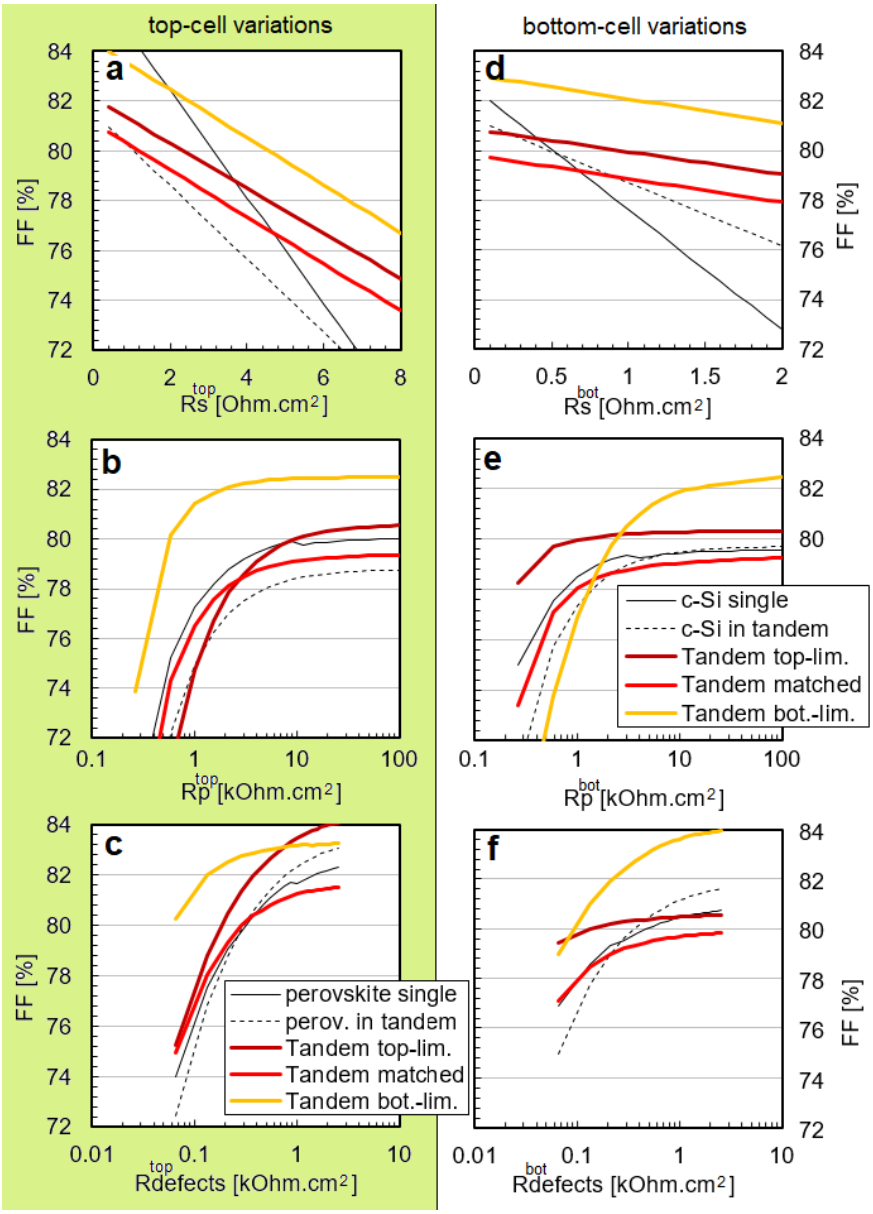

FIG. 4 Fill-factor change upon variation of the series (a,d), parallel (b,e) or defect (c,f) resistance in the perovskite (a-c) or c-Si (d-f) cell in single-junction, single-junction in tandem or tandem with three different matching conditions.

shunting in the top-cell, preserving FF > 82% even for Rp^{top} as low as 2 kOhm cm^2. Using such low Rp^{top} for a top-limited device would contrariwise lead to a 3% FF drop compared to a non-shunted device (Fig. 4b dark red).

Similar observation can be made upon modification of the local defects (Fig. 4c and f), which has little impact in a reasonable range if changed in the non-limiting subcell. Again, FF values above 82% can be maintained for bottom-limited devices for a large range of variations of the defect resistance of the top cell (Fig. 4c). Comparing the influence of this resistance on single-junctions (black lines) and matched-tandem devices (red lines), it can be seen that the tandem device is similarly impacted as the top-cell and bottom cell (Fig. 4c and f). This is also the case for the parallel resistance (Fig. 4b and e). There seems to be a relatively good correlation between the FF of the tandem device and the one of the sub-cell for these particular cases. Correlating the FF of the tandem device to the one of each individual subcell is the focus of next section.

Fig. 5 shows the FF of the tandem device as a function of the FF of the relevant single-junction device upon modifying each one of the resistance discussed previously. We consider a bottom-limited (a,d), current-matched (b,e), or top-limited (c,f) tandem device. Again, a striking observation is that no obvious correlation is appearing at first glance, confirming the idea that the FF of a tandem device is not correlated in general to the FF of each constituent subcells. However, as discussed in previous paragraph, a linear correlation with close to unit slope is seen for current-matched tandem devices when modifying the defects or parallel resistances (Fig. 5b and e). The relatively modest FF of the reference single-junction perovskite devices with respect to their Voc, caused by local inhomogeneities or other bulk defects and hence corresponding to

the defect parameter of our model, is also significantly contributing to the relatively low FF of experimental tandem devices as reported in Ref [12].

Concerning series resistance (Fig. 5a and d), it has remarkably little impact on the FF of the tandem device despite its strong influence on the FF of each individual subcell. Although this is

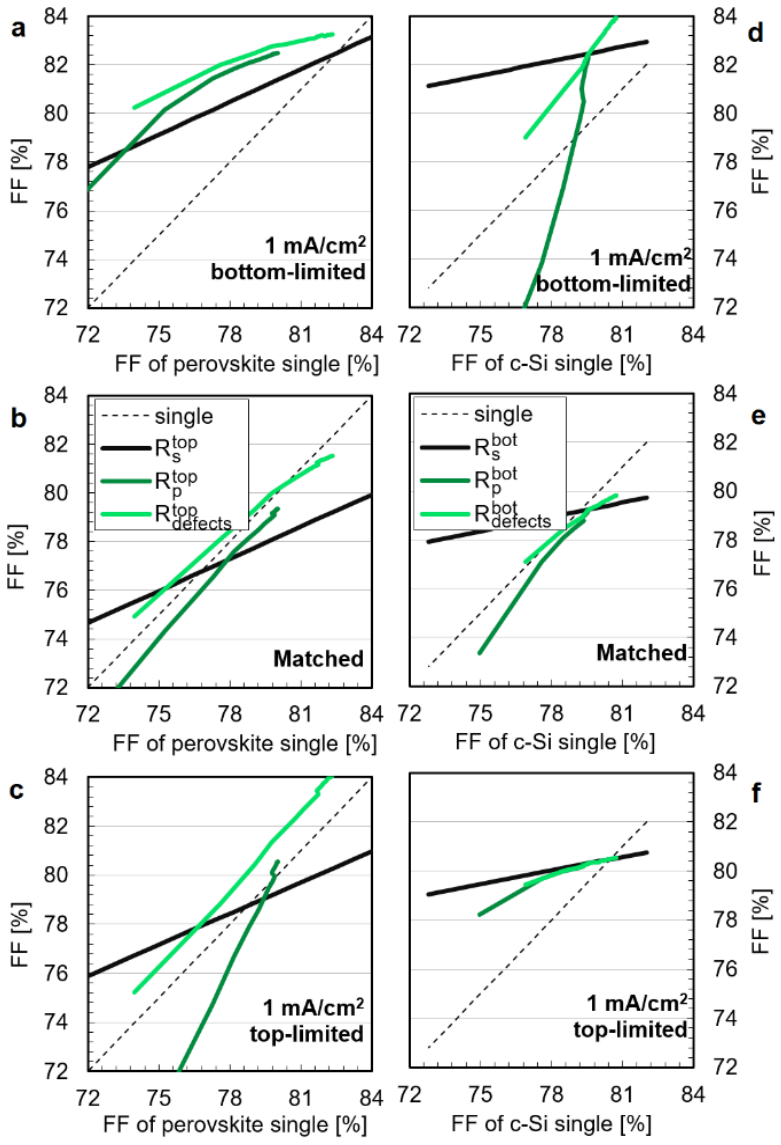

Figure 5 a-c) FF of a perovskite-silicon tandem device as a function of the FF of the reference perovskite single-junction cell when changing the series resistance, parallel resistance, or defect resistance for a top-limited (a), matched (b) or bottom-limited (c) device. d-f) Same as (a-c) but modifying the crystalline-silicon bottom cell.

redundant with the preceding discussion about the role of the device impedance, it is worth highlighting since series resistance is a major cause of FF variation in c-Si devices. Observing the relatively flat thick black lines in Fig. 5 d-f, it can be concluded that a minor change in the FF of a c-Si cell, if related to the series resistance, will go unnoticed in the tandem device.

Another important observation, already made previously, is that a change in the defect resistance or parallel resistance of the top cell will affect more strongly a top-limited tandem device than a bottom-limited one. This can be observed from the much steeper green curves in Fig. 5c than Fig. 5a. Again, bottom limitation appears as an efficient way of mitigating the effect of defects in the perovskite subcell to achieve high-FF tandem devices. Note that a reduction in parallel resistance of the bottom cell in that configuration would strongly impact the tandem device performance (yellow curve in Fig. 4e). This is however unlikely to occur in realistic devices since wafer-based technology is little prone to ohmic shunting. Also, it should be noted that in the very simplified model used here, the effects of lateral current flows which occur in real devices are neglected. Since these might be different between the tandem and single-junction devices, the relationships of Fig. 5 would deviate. Overall, these should be viewed as general trend lines rather than accurate simulations of a real device which would require more elaborate 3D modelling.

Finally, as a case-study, we compare in the following two designs of the bottom cell yielding a similar 24% efficiency as single junctions: a silicon heterojunction solar cell (SHJ) and what could be an efficient device based on the next generation of architectures coming after the passivated-emitter-and-rear-cell architecture (PERC+).[28] Parameters chosen in these simple simulations are by design arbitrary, yet they reflect the main differences between SHJ and PERC+: SHJ typically reaches higher voltage than PERC+, yet lower current and lower fill-

factor through higher series resistance. The resulting solar cell characteristics for single-junction and tandem configurations are shown in Table 3.

Table 3 Solar cell parameters simulated for either a SHJ or PERC configuration of the c-Si device

	SHJ			PERC+		
	single	bottom	tandem	single	bottom	tandem
Voc (mV)	738	720	1782	692	670	1732
Jsc (mA/cm^2)	40.11	19.95	19.93	42.00	19.96	19.93
FF (%)	81.09	82.01	79.89	82.62	82.51	80.05
Efficiency (%)	**24.02**	**11.78**	**28.38**	**24.01**	**11.04**	**27.64**
Roc (Ω.cm^2)	1.29	2.03	5.65	0.74	1.46	5.08
Rsc (kΩ.cm^2)	9.48	17.79	26.35	9.44	18.10	26.29

The simple simulations used here enable to evidence that these two strategies, yielding identical performance as single-junction devices (24.0% efficiency), are not equivalent when used as bottom cells of a tandem device: efficiency is simulated to drop from 28.4% to 27.6% when replacing a SHJ bottom cell by a PERC+ bottom cell. This stems from two main effects. First, the main limitation of the SHJ approach, parasitic absorption of short-wavelength light in the amorphous silicon layers, vanishes in tandem configuration since short-wavelength light is absorbed in the top-cell before reaching the bottom cell. Both devices are thus set to the same photogenerated current in bottom-cell configuration. Second, the other main limitation of SHJ is the relatively high series resistance (which stems from contact resistance from the wafer to the laterally conducting transparent electrode, low conductivity of low-curing-temperature silver paste, and lateral transport in the transparent electrode). Although the series resistances for both cases were maintained when incorporation as a bottom cell (which is arguable since the lateral transport and metallization in tandem configuration are expected to be similar for both

architecture), the difference in series resistance impacts much less the tandem device than the single junction, as discussed previously. Hence, FF difference between SHJ and PERC+ vanishes from 1.5% to less than 0.2%, as visible from the relatively flat colored lines in FIG. 4d or black line in Figure 5e. On the other hand, the higher voltage of the SHJ approach benefits fully to the tandem structure (even contributing to lowering the impact of series resistance from the top cell). Interestingly, simulation of a tandem device relying on the recently announced 24.6%-efficient device using a TOPCon approach[29] yields an efficiency of 28.29% only. This is 0.1% below the one obtained with the SHJ device, in spite of the latter having a 0.6% lower single-junction efficiency. This reflects the general trend that, in view of an application in tandem devices, a high-fill-factor silicon device (requiring extremely low series resistance) is not necessary but high open-circuit voltage (requiring extremely good passivation) is of paramount importance.

In conclusion, we simulated the influence of series resistance, parallel resistance and local defects in each subcell of a tandem device on the fill-factor of this tandem device as well as of its subcell. We observed that no general correlation between the FF of the single-junction device and the one of the tandem device can be made. In particular, series resistance is strongly affecting FF of the single junction devices (especially the c-Si bottom cell showing a lower impedance at maximum power point) yet is relatively harmless for the FF of the tandem device. Concerning the effect of defects and parallel resistance, the current matching is shown to have a strong impact, and the FF of the tandem device is shown to be little affected by changes on the non-limiting subcell. On the other hand, the FF of a current-matched tandem device does correlate linearly with the FF of individual subcells. Eventually, modifications of the parallel resistance of the limiting subcell will affect the FF of the tandem device more strongly than the FF of the corresponding single junction. Overall, bottom-limitation appears to be an efficient

way to maintain high FF values in most realistic situations. Looking at realistic high-efficiency silicon devices, the improved FF stemming from reduced series resistance of novel contacting strategies in silicon devices appear of little value in the context of tandem devices. On the other hand, reaching high open-circuit voltages is needed to fully benefit from tandem devices, suggesting thus that the silicon heterojunction architecture is currently the most promising technology to reach high efficiencies with silicon-based tandem-device.

ASSOCIATED CONTENT

Supporting Information. The Supporting Information is available free of charge on the ACS Publications website at DOI: XXXX

Experimental validation of the simulation model, discussion of improvement routes for experimental perovskite/silicon devices, and simulated current-voltage curves for tandem devices for various matching conditions.

AUTHOR INFORMATION

Mathieu.boccard@epfl.ch, https://www.epfl.ch/labs/pvlab/

ACKNOWLEDGMENT

The authors thank Quentin Jeangros and Florent Sahli for fruitful discussions, and M. Boccard acknowledges the Swiss National Science Foundation under Ambizione Energy Grant ICONS (PZENP2_173627).

REFERENCES

(1) Ventosinos, F.; Klusacek, J.; Finsterle, T.; Kunzel, K.; Haug, F. J.; Holovsky, J. Shunt Quenching and Concept of Independent Global Shunt in Multijunction Solar Cells. *IEEE J. Photovoltaics* **2018**, *8* (4), 1005–1010. https://doi.org/10.1109/JPHOTOV.2018.2828850.

(2) Burdick, J.; Glatfelter, T. Spectral Response and I-V Measurements of Tandem Amorphous-Silicon Alloy Solar Cells. *Sol. Cells* **1986**, *18* (3–4), 301–314. https://doi.org/10.1016/0379-6787(86)90129-8.

(3) Das, C.; Xiang, X.; Deng, X. Measurement of Component Cell Current-Voltage Characteristics in a Tandem- Junction Two-Terminal Solar Cell. In *High efficiency and high rate deposited amorphous silicon-based solar cells*; 2006; pp 73–80.

(4) Tsuno, Y.; Hishikawa, Y.; Kurokawa, K. Separation of the I-V Curve of Each Component Cell of Multi-Junction Solar Cells. *Conf. Rec. IEEE Photovolt. Spec. Conf.* **2005**, No. V, 1476–1479. https://doi.org/10.1109/pvsc.2005.1488421.

(5) Kurtz, S. F.; Emery, K.; Olson, J. M. METHODS FOR ANALYSIS OF TWO-JUNCTION , TWO-TERMINAL PHOTOVOLTAIC DEVICES. In *1st World Conference on Photovoltaic Energy Conversion*; 1994; pp 1733–1737.

(6) Morel, D.; Wieting, R.; Mitchell, K. No Title. In *First International Photo- voltaic Science and Engineering Corororence, Kobe, Japan, PVSEC-1*; 1984; pp 567–570.

(7) Faine, P.; Kurtz, S. R.; Riordan, C.; Olson, J. M. The Influence of Spectral Solar Irradiance Variations on the Performance of Selected Single-Junction and Multijunction Solar Cells. *Sol. Cells* **1991**, *31* (3), 259–278. https://doi.org/10.1016/0379-6787(91)90027-M.

(8) Nakajima, A.; Ichikawa, M.; Sawada, T.; Yoshimi, M.; Yamamoto, K. Spectral Characteristics of Thin-Film Stacked-Tandem Solar Modules. *Jpn. J. Appl. Phys.* **2004**, *43* (10), 7296–7302. https://doi.org/10.1143/JJAP.43.7296.

(9) Ulbrich, C.; Zahren, C.; Gerber, A.; Blank, B.; Merdzhanova, T.; Gordijn, A.; Rau, U. Matching of Silicon Thin-Film Tandem Solar Cells for Maximum Power Output. *Int. J. Photoenergy* **2013**, *2013*, 314097.

(10) Bonnet-Eymard, M.; Boccard, M.; Bugnon, G.; Sculati-Meillaud, F.; Despeisse, M.; Ballif, C. Optimized Short-Circuit Current Mismatch in Multi-Junction Solar Cells. *Sol. Energy Mater. Sol. Cells* **2013**, *117* (0), 120–125. https://doi.org/10.1016/j.solmat.2013.05.046.

(11) Köhnen, E.; Jošt, M.; Morales-Vilches, A. B.; Tockhorn, P.; Al-Ashouri, A.; Macco, B.; Kegelmann, L.; Korte, L.; Rech, B.; Schlatmann, R.; et al. Highly Efficient Monolithic Perovskite Silicon Tandem Solar Cells: Analyzing the Influence of Current Mismatch on Device Performance. *Sustain. Energy Fuels* **2019**, *3* (8), 1995–2005. https://doi.org/10.1039/c9se00120d.

(12) Sahli, F.; Werner, J.; Kamino, B. A.; Bräuninger, M.; Monnard, R.; Paviet-Salomon, B.; Barraud, L.; Ding, L.; Leon, J. J. D.; Sacchetto, D.; et al. Fully Textured Monolithic Perovskite/Silicon Tandem Solar Cells with 25.2% Power Conversion Efficiency. *Nat. Mater.* **2018**, *17* (9), 820. https://doi.org/10.1038/s41563-018-0115-4.

(13) Mazzarella, L.; Lin, Y. H.; Kirner, S.; Morales-Vilches, A. B.; Korte, L.; Albrecht, S.; Crossland, E.; Stannowski, B.; Case, C.; Snaith, H. J.; et al. Infrared Light Management Using a Nanocrystalline Silicon Oxide Interlayer in Monolithic Perovskite/Silicon

Heterojunction Tandem Solar Cells with Efficiency above 25%. *Adv. Energy Mater.* **2019**, *9* (14), 1803241. https://doi.org/10.1002/aenm.201803241.

(14) Chen, B.; Yu, Z.; Liu, K.; Zheng, X.; Liu, Y.; Shi, J.; Spronk, D.; Rudd, P. N.; Holman, Z.; Huang, J. Grain Engineering for Perovskite/Silicon Monolithic Tandem Solar Cells with Efficiency of 25.4%. *Joule* **2019**, *3* (1), 177–190. https://doi.org/10.1016/j.joule.2018.10.003.

(15) Bush, K. A.; Manzoor, S.; Frohna, K.; Yu, Z. J.; Raiford, J. A.; Palmstrom, A. F.; Wang, H. P.; Prasanna, R.; Bent, S. F.; Holman, Z. C.; et al. Minimizing Current and Voltage Losses to Reach 25% Efficient Monolithic Two-Terminal Perovskite-Silicon Tandem Solar Cells. *ACS Energy Lett.* **2018**, *3* (9), 2173–2180. https://doi.org/10.1021/acsenergylett.8b01201.

(16) Bush, K. A.; Palmstrom, A. F.; Yu, Z. J.; Boccard, M.; Cheacharoen, R.; Mailoa, J. P.; McMeekin, D. P.; Hoye, R. L. Z.; Bailie, C. D.; Leijtens, T.; et al. 23.6%-Efficient Monolithic Perovskite/Silicon Tandem Solar Cells With Improved Stability. *Nat. Energy* **2017**, *2* (4), 1–7. https://doi.org/10.1038/nenergy.2017.9.

(17) Wu, Y.; Yan, D.; Peng, J.; Duong, T.; Wan, Y.; Phang, S. P.; Shen, H.; Wu, N.; Barugkin, C.; Fu, X.; et al. Monolithic Perovskite/Silicon-Homojunction Tandem Solar Cell with over 22% Efficiency. *Energy Environ. Sci.* **2017**, *10* (11), 2472–2479. https://doi.org/10.1039/c7ee02288c.

(18) Nogay, G.; Sahli, F.; Werner, J.; Monnard, R.; Boccard, M.; Despeisse, M.; Haug, F. J.; Jeangros, Q.; Ingenito, A.; Ballif, C. 25.1%-Efficient Monolithic Perovskite/Silicon Tandem Solar Cell Based on Ap-Type Monocrystalline Textured Silicon Wafer and High-

Temperature Passivating Contacts. *ACS Energy Lett.* **2019**, *4*, 844–845.

(19) Merten, J.; Asensi, J. M.; Voz, C.; Shah, A. V.; Platz, R.; Andreu, J. Improved Equivalent Circuit and Analytical Model for Amorphous Silicon Solar Cells and Modules. *IEEE Trans. Electron Devices* **1998**, *45* (2), 423–429. https://doi.org/10.1109/16.658676.

(20) Munoz, D.; Razongles, G.; Coignus, J.; Merten, J. Novel Equivalent Circuit for Heterojunction Cells and Diagnostic Method Based on Variable Illumination Measurements (VIM). In *27th European Photovoltaic Solar Energy Conference Exhibition*; 2012.

(21) Kassis, A.; Saad, M. Analysis of Multi-Crystalline Silicon Solar Cells at Low Illumination Levels Using a Modified Two-Diode Model. *Sol. Energy Mater. Sol. Cells* **2010**, *94* (12), 2108–2112. https://doi.org/10.1016/j.solmat.2010.06.036.

(22) Mcintosh, K. R. Lumps, Humps and Bumps: Three Detrimental Effects in the Current-Voltage Curve of Silicon Solar Cells. *PhD thesis Univ. New South Wales* **2001**, No. September, 63–73. https://doi.org/10.13140/RG.2.2.19197.26083.

(23) Hernando, F.; Gutierrez, J. R.; Bueno, G.; Recart, F.; Rodriguez, V. Humps, a Surface Damage Explanation. In : *2nd. World Conference and Exhibition on Photovoltaic Solar Energy Conversion*; 1998; pp 1321–1323.

(24) Despeisse, M.; Boccard, M.; Bugnon, G.; Cuony, P.; Soderstrom, T.; Parascandolo, G.; Stuckelberger, M.; Charriere, M.; Lofgren, L.; Battaglia, C.; et al. Low-Conductivity Doped Layers for Improved Performance of Thin Film Silicon Solar Cells on Highly Textured Substrates. In *25th European Photovoltaic Solar Energy Conference and Exhibition / 5th World Conference on Photovoltaic Energy Conversion, 6-10 September 2010, Valencia,*

Spain; 2010; pp 2793–2797. https://doi.org/10.4229/25thEUPVSEC2010-3CO.13.4.

(25) Bugnon, G.; Söderström, T.; Nicolay, S.; Ding, L.; Despeisse, M.; Hedler, A.; Eberhardt, J.; Wachtendorf, C.; Ballif, C. LPCVD ZnO-Based Intermediate Reflector for Micromorph Tandem Solar Cells. *Sol. Energy Mater. Sol. Cells* **2011**, *95* (8), 2161–2166. https://doi.org/10.1016/j.solmat.2011.03.018.

(26) Sahli, F.; Kamino, B. A.; Werner, J.; Bräuninger, M.; Paviet-Salomon, B.; Barraud, L.; Monnard, R.; Seif, J. P.; Tomasi, A.; Jeangros, Q.; et al. Improved Optics in Monolithic Perovskite/Silicon Tandem Solar Cells with a Nanocrystalline Silicon Recombination Junction. *Adv. Energy Mater.* **2018**, *8* (6), 1701609. https://doi.org/10.1002/aenm.201701609.

(27) Cuony, P. Optical Layers for Thin-Film Silicon Solar Cells. *EPFLThesis* **2011**, *5190*, 1–127.

(28) Tous, L.; Choulat, P.; Singh, S.; John, J.; Aleman, M.; Fırat, M.; Duerinckx, F.; Szlufcik, J. Efficiency Roadmaps for Industrial Bifacial PPERC and NPERT Cells. In *15th International Conference on Concentrator Photovoltaic Systems (CPV-15)*; AIP Publishing, 2019; Vol. 2149, p 120001. https://doi.org/10.1063/1.5123883.

(29) Chen, Y.; Chen, D.; Altermatt, P. P.; Xu, G.; Wang, Z.; Liu, C.; Zou, Y.; He, Y.; Wang, Y.; Gong, J.; et al. > 25 % LARGE-AREA INDUSTRIAL SILICON SOLAR CELL : LEARNING FROM. In *36th European PV Solar Energy Conference and Exhibition*; 2019.